

Article

Molecular Structure, Luminescent and DFT Computational Studies of Two Novel Eu (III) β -diketonate Complexes

Haifeng Shao ¹, Yanjun Hou ^{1,*}, Jinyuan Bai ¹, and Haijun Niu ^{2,*}

¹ School of Chemistry and Materials Science, Heilongjiang University, Harbin 150080, China; houyj@hlju.edu.cn

² Key Laboratory of Chemical Engineering Process and Technology for High-efficiency Conversion, College of Heilongjiang Province, Harbin 150080, China; haijunniu@hotmail.com

* Correspondence: houyj@hlju.edu.cn (Y.H.); haijunniu@hotmail.com (H.N.); Tel.: +86-451-86609135 (Y.H. & H.N.)

Abstract: In this paper, the synthesis of two novel luminescent Eu³⁺ ion complexes [Eu(TFT)₃(phen) (1) and Eu(TFT)₃(bpy)·Hex (2)] based on the combination of 2-(2,2,2-trifluoroethyl)-1-tetralone (TFT), containing n-donor ligands (1,10-phenanthroline or 2,2'-Bipyridine) and Eu³⁺ ion is reported herein, and their structural features are discussed on the basis of X-ray crystallographic and thermal analyses. We observed that the ligands transfer energy effectively to the metal center by fluorescence, IR and UV spectrograms studies. The structures and properties of complexes 1-2 were optimized by the DFT theoretical calculation, and the calculation results were consistent with the experimental X-ray structure data and spectral analysis.

Keywords: TFT; complexes; luminescent; synthesis; Density functional theory (DFT)-computation

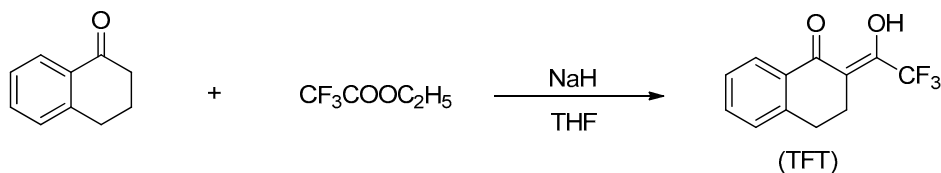
1. Introduction

As is known to all, lanthanide ions play a significant role on the basis of their peculiar luminescent properties in the field of optical research [1]. However, Ln³⁺ ions are unable to generate efficient luminescence emission under direct excitation because the 4f–4f transitions of lanthanide ions are spin forbidden [2], which results in free lanthanide ions have a weak luminescence merely. For this point, the design of lanthanide coordination compounds have attracted particular attention in order to improve luminescent properties of lanthanide ions. In this context, scientists consistently synthesize new molecular structures in order to study finely fluorescence system in recent years. In particular, lanthanide organic complexes [3], such as β -diketonate Ln³⁺ complexes [4], have great potential application in amplifiers for fluorescent materials [5], biological probes [6], and analytical sensors [7] in virtue of sharp fluorescence emissions and high quantum efficiencies. In our preliminary work, we designed a β -diketonate-type Ligand, 2-(2,2,2-trifluoroethyl)-1-tetralone (TFT) act as organic chelating agents of the trivalent Eu³⁺ ion, which formed a tris- β -diketonate (Eu³⁺) salt in the end. Then, the tris- β -diketonate (Eu³⁺) salts combined with 1,10-phenanthroline (phen) or 2,2'-Bipyridine (bpy) on the basis of coordination chemistry principle, respectively, which may increase the light absorption cross-section of metal complex via ligands transfer energy to the central Ln³⁺ ion. Furthermore, there are two key reasons for our designing scheme. On one hand, TFT is able to compose firm coordination compound with Eu³⁺ ions, and enhance the luminescence intensity due to the effect of its π - π^* transition [8]. The presence of fluorinated groups also enhances luminescent property and stable performance of complexes effectively because of its strong

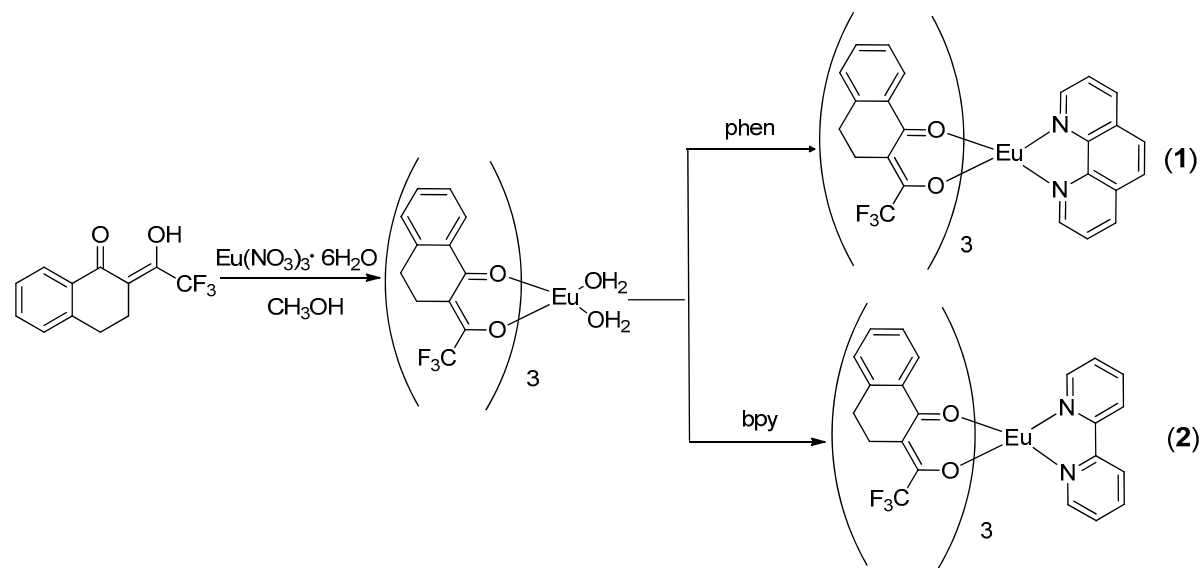
electron-withdrawing function and oxidative stability, respectively [9]. On the other hand, the auxiliary ligands, such as phen and bpy play an important role in increasing luminous emission intensity and inhibiting the fluorescence quenching by an intramolecular energy transfer process from ancillary ligands to central metal ion, the so-called “synergistic effect” [10]. The structure and property analysis of complexes are described in more detail below.

2. Results and Discussion

As shown in Scheme I, the ligand 2-(2,2,2-trifluoroethyl)-1-tetralone has been synthesized by classical Claisen condensation of 1-tetralone with ethyl trifluoroacetate in the THF containing NaH. According to the synthetic method of relevant literature [11], we synthesized the target compound with excellent yield. The reaction conditions would be described in detail in a follow-up Experimental Section. Here, we designed the tris- β -diketonate (Eu^{3+}) salt, $\text{Eu}(\text{TFT})_3(\text{H}_2\text{O})_2$ [TFT = 2-(2,2,2-trifluoroethyl)-1-tetralone]. In order to seek target complexes with outstanding luminescent properties, we focused on attractive 1,10-phenanthroline or 2,2'-Bipyridine as ancillary ligand, reacted with $\text{Eu}(\text{TFT})_3(\text{H}_2\text{O})_2$ to generate complexes **1-2** in methanol (Scheme II). Herein, we report the successful assembly of two new tris- β -diketonate Eu(III) complexes, namely $\text{Eu}[\text{2-(2,2,2-trifluoroethyl)-1-tetralone}]_3\text{phenanthroline}$ and $\text{Eu}[\text{2-(2,2,2-trifluoroethyl)-1-tetralone}]_3\text{bipyridine}$, and reveal the crystal structures of them. The crystal data and refinement details are summarized in Table 1.



Scheme I. Synthesis of the TFT.



Scheme II. Synthesis of complexes **1-2**.

Table 1. Crystal Data and Structure Refinement for Complex 1-2

Parameter	Complex 1	Complex 2
empirical formula	C48 H30 Eu F9 N2 O6	C49 H39 Eu F9 N2 O6
formula weight	1053.70	1074.78
temperature/K	296(2)	296(2)
Color	Buff	Buff
crystal system	monoclinic	monoclinic
space group	P21/n	P21/n
<i>a</i> /Å	21.005(2)	12.0336(16)
<i>b</i> /Å	9.6340(9)	21.134(3)
<i>c</i> /Å	22.989(2)	19.0963(17)
α (deg)	90.000	90.000
β (deg)	105.1550(10)	110.757(6)
γ (deg)	90.000	90.000
<i>V</i> (Å ³)	4490.3(7)	4541.3(10)
<i>Z</i>	4	4
ρ (g cm ⁻³)	1.559	1.572
μ (mm ⁻¹)	1.485	1.470
<i>F</i> (000)	2096.0	2156.0
R1, [I > 2 σ (I)]	0.0524	0.0430
wR2, [I > 2 σ (I)]	0.1174	0.0961
R1, (all data)	0.1240	0.0828
wR2, (all data)	0.1475	0.1134
CCDC	1484014	1524434

2.1. Molecular Structure of the Complex 1

The molecular structure of complex 1 [Eu(TFT)₃(phen)] is revealed by Single crystal X-ray diffraction studies, which crystallizes in the the monoclinic crystal system with a space group of P21/n. The asymmetric unit of complex 1 is composed of one independent Eu³⁺ ion, three deprotonated ligands (TFT), and one phen. The ligand (TFT) and phen serve as two bidentate ligands and chelate the Eu³⁺ ion on coordination chemistry principle (Figure 1a, Figure S1). Each Eu³⁺ ion centre adopts a distorted hexahedron, coordinated by six oxygen atoms from three carbonyl groups (O₁, O₃, O₅), three methoxy groups (O₂, O₄, O₆) of three ligands (TFT) and two nitrogen atoms (N₁, N₂) from one phen (Figure 1b). The selected bond lengths for complex 1 are shown in Table 2, and the selected bond angles (°) are in Table S1. The average bond length of the Eu–O (TFT oxygen atoms) and Eu–N (phen nitrogen atoms) is 2.347 Å and 2.588 Å, respectively. The average length of the Eu–N bond (2.588 Å) with the nitrogen atoms from phen is substantial longer indicating a weak interaction. In other words, the TFT ligand is more stable binding to the central metal ion, which is due to the strong interaction of Eu³⁺ ion and oxygen atoms.

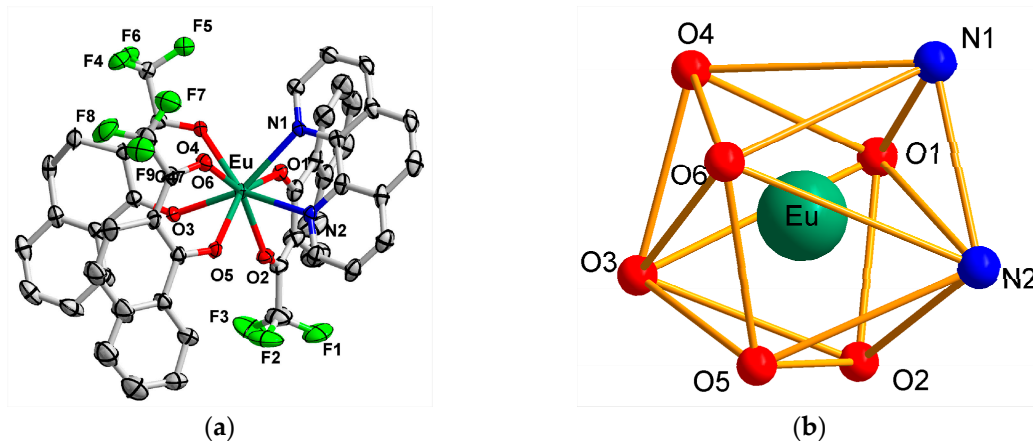


Figure 1. Molecular structure for $\text{Eu}(\text{TFT})_3(\text{phen})$, the ORTEP drawing (15% probability level) (a); and simplified stick exhibition (b).

Table 2. Selected bond lengths (\AA) in $\text{Eu}(\text{TFT})_3(\text{phen})$

Bond Lengths	
Eu(1) -O1	2.347(4)
Eu(1)-O2	2.351(5)
Eu(1)-O3	2.324(4)
Eu(1)-O4	2.347(4)
Eu(1)-O5	2.354(4)
Eu(1)-O6	2.358(4)
Eu(1)-N1	2.590(5)
Eu(1)-N2	2.586(5)

Each asymmetric unit of complex **1** can form a more stable structure via several hydrogen bonds interaction between the atoms, as shown in Figure 2. These hydrogen bonds (C-H...F, C-H...O) are composed of F, O and H atoms from TFT and phen ligands, which is an important factor in enhancing the thermal stability and stabilizing the crystal structure for the complex **1** [12]. Within these hydrogen bonds, the F(4) and F(6) atoms are interconnected with a same atom H(33B), which form the C(33)-H(33B)...F(4) and C(33)-H(33B)...F(6), respectively. It's worth mentioning that hydrogen bonds C(1)-H(1)...O(4) and C(12)-H(12)...O(5) are composed of [O(4), O(5)] from TFT and [H(1), H(12)] from phen. The ligands TFT and phen are interconnected via weak hydrogen bonds C(1)-H(1)...O(4) and C(12)-H(12)...O(5) contacts enhancing stability of crystal structure. In this context, The success ratio of cultivation of single crystal is also significantly higher than β -diketonate (Eu^{3+}) salt $[\text{Eu}(\text{TFT})_3(\text{H}_2\text{O})_2]$ during the practical tests. The length and angle of hydrogen bonds are listed in Table S2.

2.2. Molecular Structure of the Complex 2

The molecular structure of the complex **2** is exhibited in Figure 3. Single crystal X-ray diffraction studies reveal that complex **2** crystallizes in the monoclinic space group $P21/n$ with $Z = 4$ and consists of neutral and mononuclear $[\text{Eu}(\text{TFT})_3\text{bpy}]$ units and solvent n-hexane. In analogy to complex **1**, the complex **2** introduces bpy instead of phen as ancillary ligand. The average bond length of the Eu-O (TFT oxygen atoms) and Eu-N (bpy nitrogen atoms) is 2.357 \AA and 2.583 \AA , which reduced 0.01 (Eu-O) and 0.005 (Eu-N) in contrast to complex **1**, respectively. The selected bond lengths for complex **2** are shown in Table 3, and the selected bond angles ($^\circ$) are in Table S3. Besides that, the π - π stacking interaction which is same as hydrogen bonding (Table S4) also has a

great significance to the stabilization of crystal structure. The molecules of complex **2** formed a 1D chained structure via the π - π stacking interaction, as shown in Figure 4. The result of the π - π bond measured was 3.898 Å.

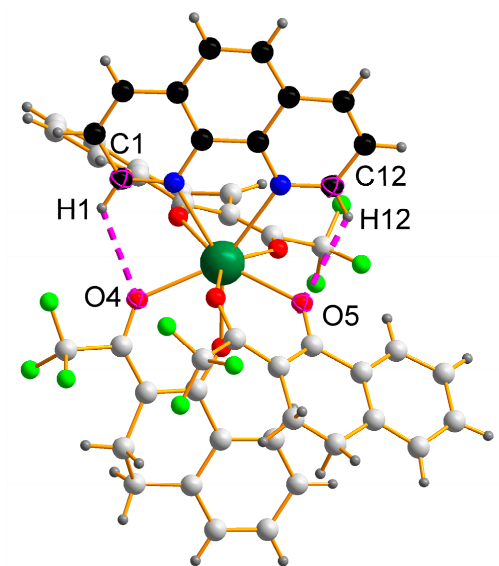


Figure 2. Intramolecular hydrogen bonding of Eu(TFT)₃(phen).

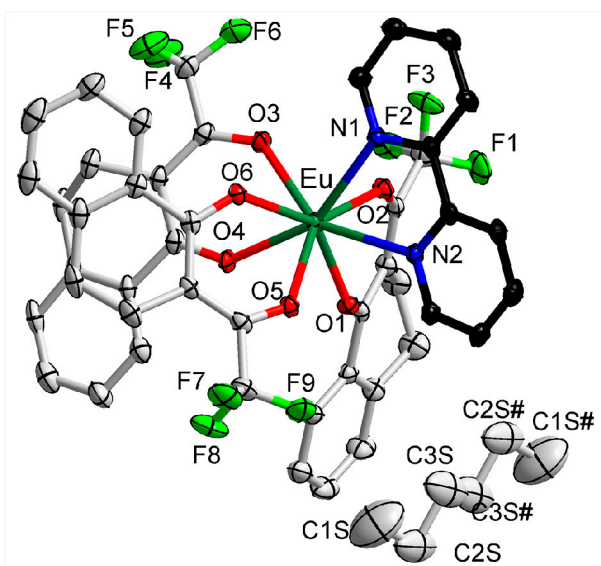


Figure 3. Molecular structure for Eu(TFT)₃(bpy)·Hex, the ORTEP drawing (15% probability level), Symmetry operator (1 - x, 1 - y, 1 - z) generates equivalent atoms that are marked with "#".

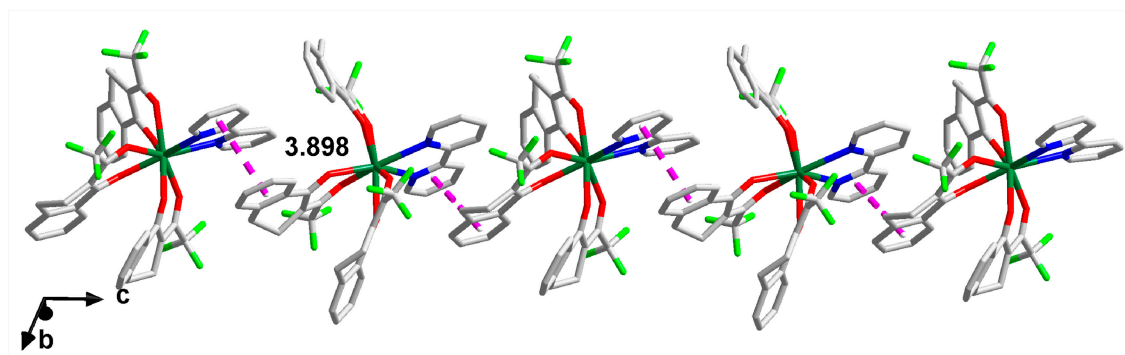


Figure 4. Complex **2** formed 1D chained structure by the π - π stacking interaction.

Table 3. Selected bond lengths (Å) in Eu(TFT)₃(bpy)·Hex

Bond Lengths		
Eu(1)-O1	2.341(3)	C(3S)-C(2S)
Eu(1)-O2	2.368(3)	C(3S)-C(3S) ^{#1}
Eu(1)-O3	2.356(3)	C(1S)-C(2S)
Eu(1)-O4	2.347(3)	
Eu(1)-O5	2.351(3)	
Eu(1)-O6	2.379(3)	
Eu(1)-N1	2.576(3)	
Eu(1)-N2	2.590(8)	

2.3. UV-Vis spectral analysis

The ultraviolet absorption spectrum of TFT, and complexes **1-2** are shown in CH₃CN solution (1×10⁻⁵ mol·L⁻¹). According to spectral (Figure 5), the absorption broad band appeared slight blue-shift from 363 nm for the TFT to 362 nm for the Na(TFT) because of β-diketonate proton transfer happened. In addition, the absorption maximum observed around 263 and 272 nm in phen and bpy respectively are due to the singlet–singlet π – π^* absorption of the ancillary ligand. As for the lanthanide(III)-cored complexes **1-2**, two sets of typical UV–Vis absorption peaks 353 and 359 nm are observed with a higher absorption intensity, which are blue-shifted compared to ligand TFT (max = 363 nm), respectively, due to the influence of TFT complexation with Eu³⁺ ion. In addition, the molar absorption coefficient values of complexes **1-2** is about 0.9 × 10⁵·L⁻¹ mol⁻¹ cm⁻¹ around 350-360 nm, which is three times higher than that for the ligand TFT base on each of the complexes consisting of three ligands.

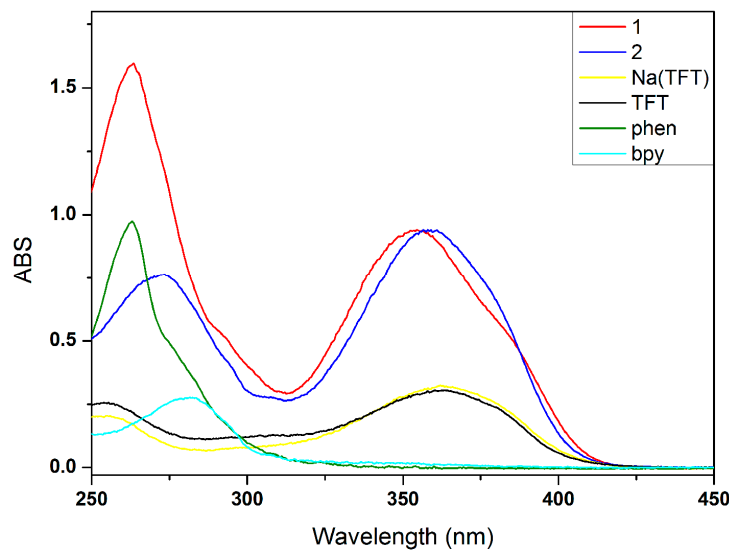


Figure 5. UV-vis absorption spectra of TFT, Na(TFT), phen, bpy and complexes **1-2** in CH₃CN solution (c = 1 × 10⁻⁵ M).

2.4. Thermal stability analysis

The thermal stabilities of the β-diketonate (Eu³⁺) salt [Eu(TFT)₃(H₂O)₂] and complexes **1-2** are analyzed with thermogarvimetric analysis (TGA) in a temperature range from 50 to 720 °C at a rate

of $10^{\circ}\text{C}\cdot\text{min}^{-1}$ under nitrogen gas atmosphere. As shown in Figure 6a, the TGA curve of $[\text{Eu}(\text{TFT})_3(\text{H}_2\text{O})_2]$ shows a weight loss of 3.4% in the temperature range $50\text{--}120^{\circ}\text{C}$, corresponds to the coordinated water molecules (calcd 3.4%) lost gradually, a weight loss of 74.2% in the temperature range $180\text{--}650^{\circ}\text{C}$, corresponds to the TFT ligands (calcd 73.8%) decomposes gradually. The TGA curve of complex **1** shows a weight loss of 85.9% in the temperature range $250\text{--}650^{\circ}\text{C}$ (Figure 6b), corresponds to the TFT and phen ligands (calcd 86.1%) decomposes gradually, while the TGA curve of complex **2** shows a weight loss of 4% in the temperature range $190\text{--}210^{\circ}\text{C}$ (Figure 6c), corresponds to the solvent n-hexane (calcd 4%) decomposes gradually, a weight loss of 76.2% in the temperature range $250\text{--}650^{\circ}\text{C}$, corresponds to the TFT and bpy ligands (calcd 76.8%) decomposes gradually. The final mass residues of complexes **1****–****2** were europium oxide. The weight-loss temperature of TFT will transfer from 180°C to 250°C when the auxiliary ligands bonded in metal ion. This result is consistent with the conclusion of hydrogen bonds analysis, the TFT ligands are interconnected with phen or bpy via weak hydrogen bonds or $\pi\text{--}\pi$ stacking enhancing stability of crystal structure.

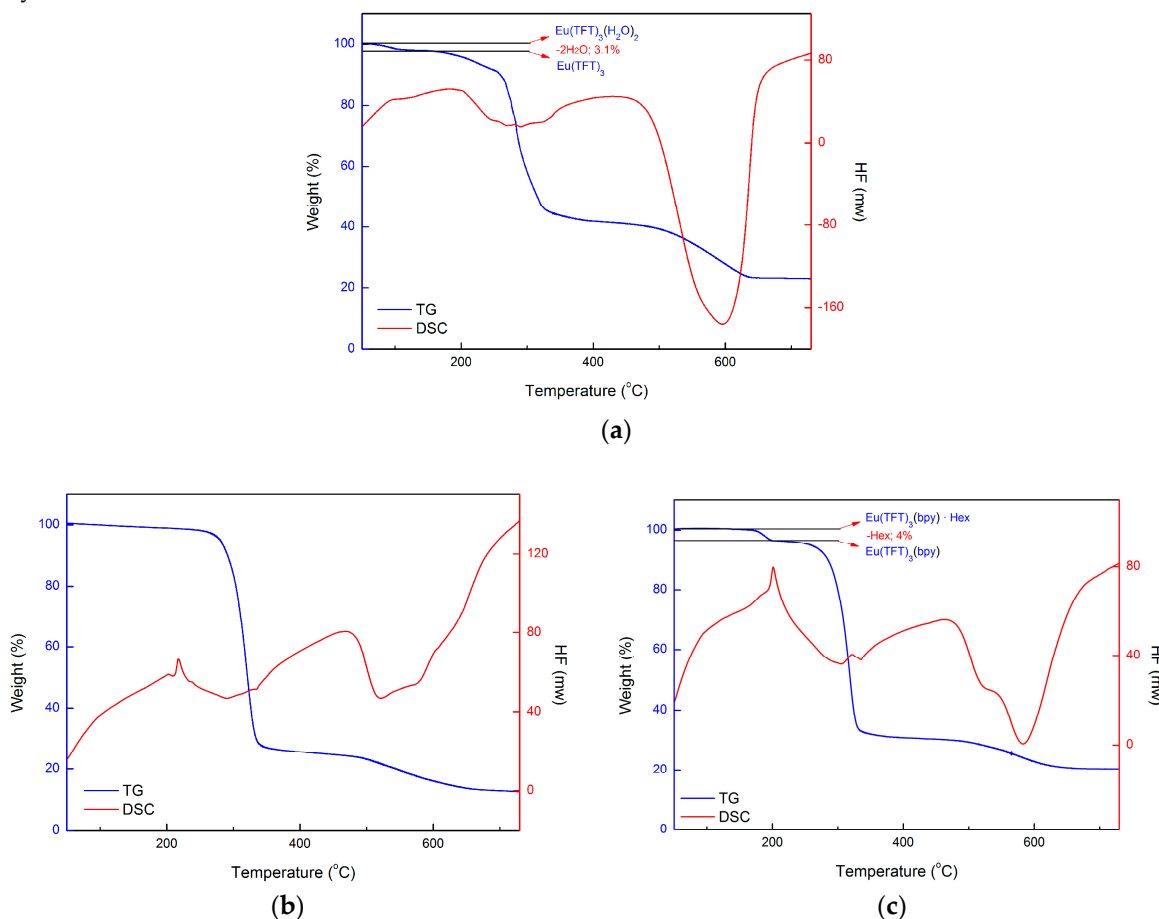


Figure 6. TGA and DSC of $\text{Eu}(\text{TFT})_3(\text{H}_2\text{O})_2$ (a), $\text{Eu}(\text{TFT})_3(\text{phen})$ (b), $\text{Eu}(\text{TFT})_3(\text{bpy})\cdot\text{Hex}$ (c). Heating rate $10^{\circ}\text{C}\cdot\text{min}^{-1}$.

2.5. Photoluminescent properties

The fluorescence spectrum of TFT and complexes **1****–****2** are shown in Figure 7. As can be seen in the emission spectra of complexes **1****–****2**, the several characteristic narrow emission bands of Eu^{3+} ion are formed upon excitation at $390\text{--}410\text{ nm}$ (Figure 7a), and corresponding to the transitions from the metal-centered $^5\text{D}_0$ excited state to the $^7\text{F}_J$ ($J = 0\text{--}4$) ground state multiple, there are $^5\text{D}_0 \rightarrow ^7\text{F}_0$

(around 580 nm), $^5D_0 \rightarrow ^7F_1$ (around 595 nm), $^5D_0 \rightarrow ^7F_2$ (around 611 nm), $^5D_0 \rightarrow ^7F_3$ (around 650 nm), and $^5D_0 \rightarrow ^7F_4$ (around 700 nm) (Figure 7b), respectively [13]. Among them, the $^5D_0 \rightarrow ^7F_2$ transition around $\lambda = 611$ nm is the highest intensity emission, which belongs to an induced electric dipole transition, thus indicating that the Eu³⁺ ion is not situated in a location with inversion center symmetry [14].

As is known, Eu(III) complexes are the most intense emitters among the lanthanide series [15], and emit red light at 605-700 nm. The blue light appeared at 450-480 nm. As can be seen in Figure 7c, the broad emission band of organic ligands ($\lambda_{em} = 468$ nm) can not be observed in field of complexes 1-2, which indicates that the ligand transfers the absorbed energy effectively to the emitting level of the Eu³⁺ ion [16]. Meanwhile we discover that the emission peak of complex 1 is far stronger than complex 2, which is due to phen has a more high efficiency of light absorption ($\lambda = 264$ nm, $\epsilon = 33\ 900\ M^{-1}\ cm^{-1}$) than bpy ($\lambda = 282$ nm, $\epsilon = 22\ 900\ M^{-1}\ cm^{-1}$), the energy of its triplet excited state (22 100 cm^{-1}) is higher than the lowest emitting level of the Eu(III) (17 500 cm^{-1}) [17]. In addition to these research, luminescent lifetime study also has a great significance. This study consequence declares that luminescence decay time of complex 1 and 2 are 27.38 and 30.73 μ s. Luminescence decay profiles been demonstrated in Figure 4(S3a, S3b).

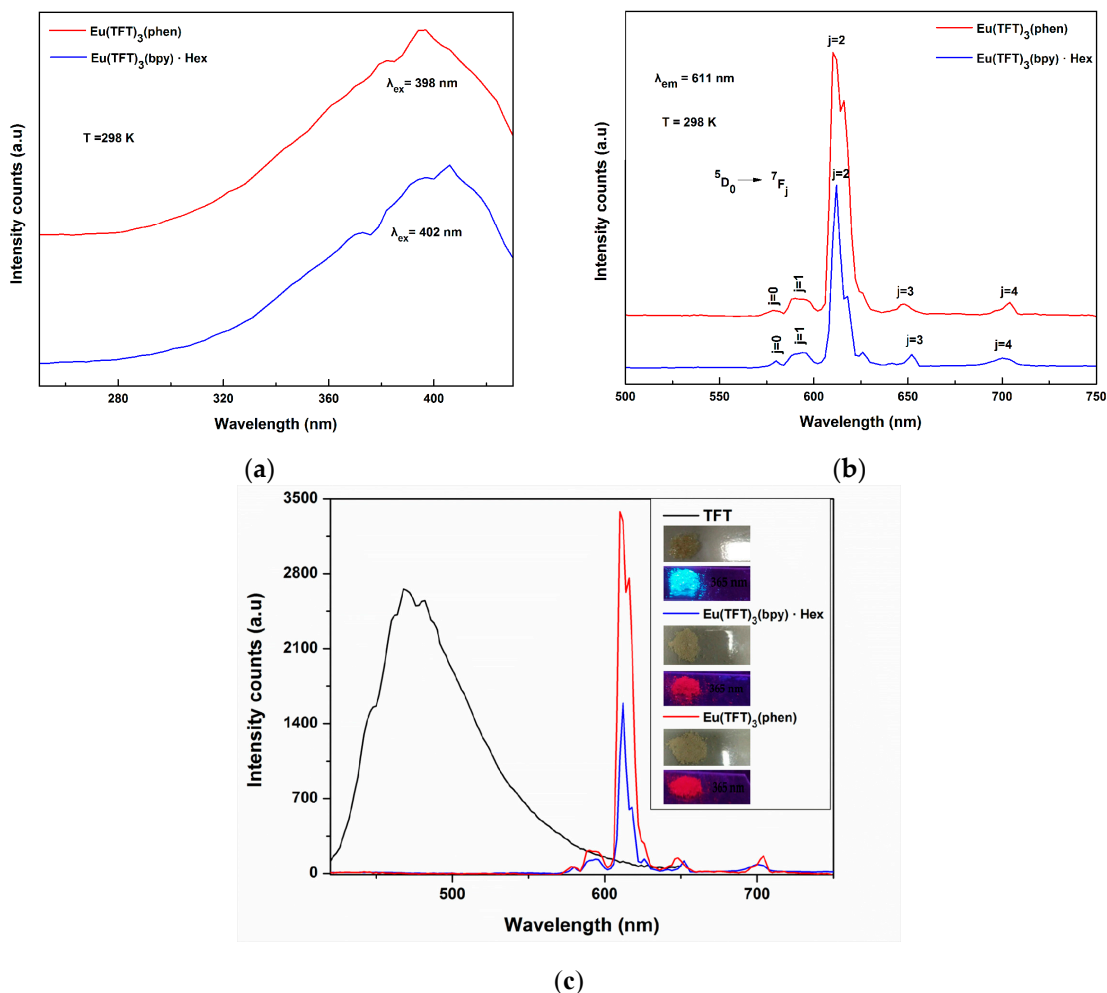


Figure 7. Excitation spectra of Eu(TFT)₃(phen) and Eu(TFT)₃(bpy)·Hex in the solid state (a); Emission spectra of Eu(TFT)₃(phen) and Eu(TFT)₃(bpy)·Hex in the solid state (b); Emission spectra of Eu(TFT)₃(phen), Eu(TFT)₃(bpy)·Hex and TFT in the solid state (c).

2.6. Computational Studies

The results of theoretical calculations for absorption properties of the complex **1** [Eu(TFT)₃(phen)] were shown in Figure 8 and Table 4. The HOMO and LUMO levels for the ground and singlet excited state of Eu³⁺ complex were -0.21 eV and -0.08 eV, -0.30 eV and 0.05 eV, respectively. The electronic cloud distribution of HOMO in singlet excited state localizes at three TFT ligands, while the one of LUMO localizes at 1,10-phenanthroline. As shown in Table 4, the lowest excitation energy of Eu³⁺ complex calculated by TD-DFT is 4.47 eV. The absorption transition is mainly due to the intraligand charge transfer (ILCT or $\pi \rightarrow \pi^*$), ligand-to-metal charge transfer (LMCT), metal-to-ligand charge transfer (MLCT) and metal centered (MC) transitions. The calculating data of S4 and S5 can explain the reason why the absorption intensity of the complex **2** is about three times as great as the ligand in the UV-vis spectra quite well.

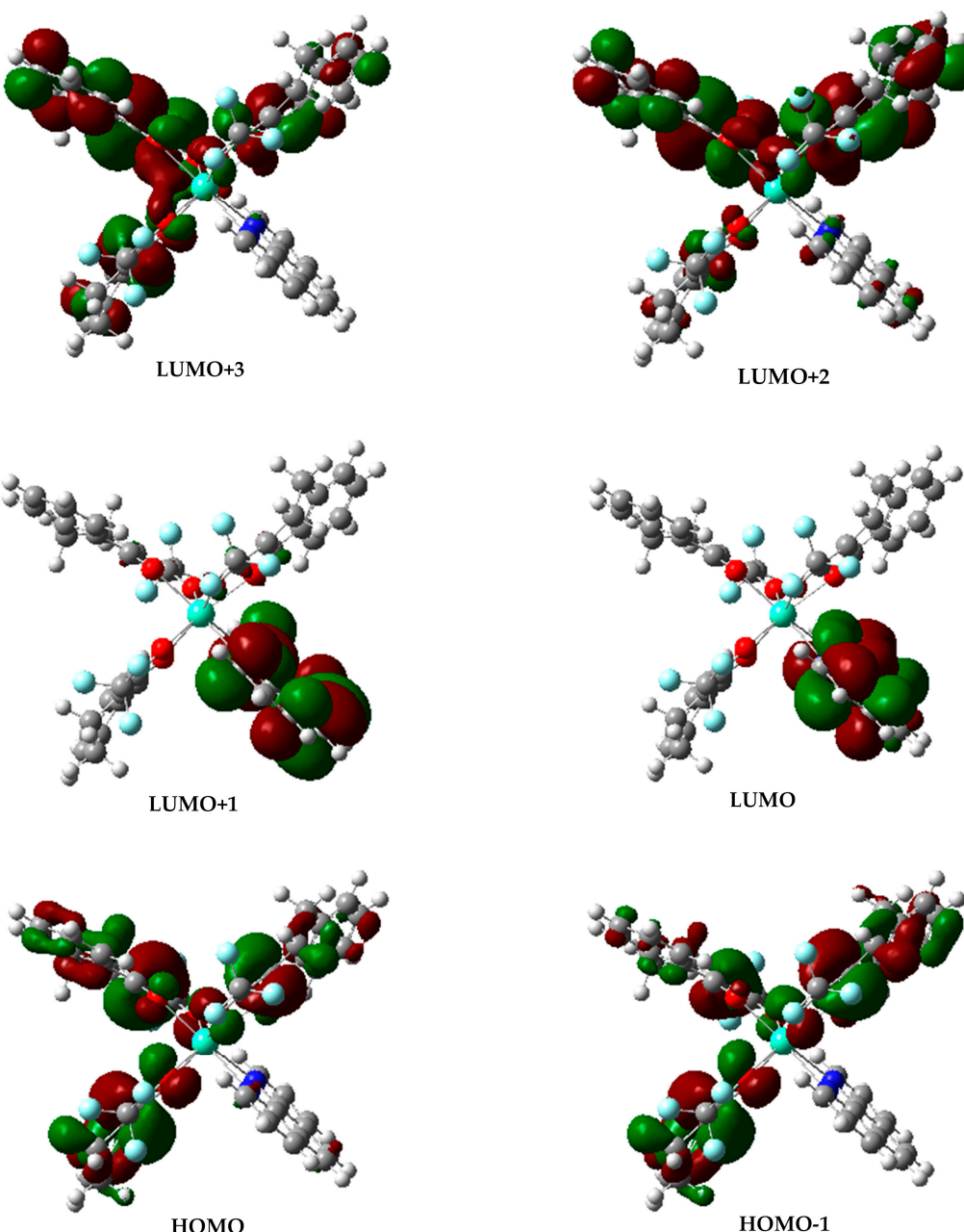


Figure 8. Spatial plots of the selected frontier molecular orbits of excited states of complex **1**.

Table 4. Absorptions of Eu complex Calculated with the TDDFT Method

complex	Sn	Confign	Cl codff	E/nm (eV)	oscillator	assignt
1	S1	H→L+2	0.2898	277.23(4.47)	0.1533	ILCT/LMCT/MLCT/MC
	S2	H→L+3	0.3316	275.69(4.49)	0.3093	ILCT
	S3	H-1→L+2	0.1572	266.16(4.66)	0.4822	ILCT/LMCT/MLCT/MC
	S4	H→L+1	0.1091	254.70(4.87)	0.0279	LMCT/MLCT/MC
	S5	H→L	0.1363	249.71(4.97)	0.0024	LMCT/MLCT/MC

3. Materials and Methods

All chemicals were purchased from Beijing Fine Chemical Co. (Beijing, China). ¹H NMR spectra were measured with a Bruker Avance III 400 MHz spectrometer in CDCl₃ solution. Fourier transform infrared (FT-IR) spectra were obtained with KBr disks in the range 4000–450 cm⁻¹. UV-Vis spectra were recorded with a Perkin-Elmer Lambda 25 spectrometer. Excitation and emission spectra were measured with an Edinburgh FLS 920 fluorescence spectrophotometer. Thermal analyses were conducted on a Perkin-Elmer STA 6000 with a heating rate of 10 °C·min⁻¹ in a temperature range from 50 to 720 °C. Single crystal diffraction intensity data were collected with a Bruker SMART APEX II X-ray diffractometer with graphite-monochromated MoK α radiation (λ = 0.71073 Å) at 296(2) K. The structures were solved by direct methods and refined on F2 by full-matrix least squares using the SHELXTL-97 program [18].

3.1. Ligand 2-(2,2,2-trifluoroethyl)-1-tetralone Syntheses

First, to a solution of 1-tetralone (0.73 g, 5.00 mmol) in THF (20 mL) was added a THF solution (10 mL) of ethyl trifluoroacetate (1.42 g, 10.00 mmol). The mixed solution was allowed to stir for 20 min. Later, NaH (0.30 g, 7.5 mmol) solids were added with vigorous stirring, and the combined solution was stirred at room temperature for 24 h in an inert atmosphere. The resulting solution was simply dumped into the distilled water and successively acidified to pH 2–3 with 6M hydrochloric acid aqueous solution. The mixed solution was extracted twice using dichloromethane (40 mL). The organic layer was separated from the water and dried overnight with anhydrous sodium sulfate. After the solvent removed by reduced pressure distillation, the oily solid is obtained. The buff solid product was isolated by column chromatography using hexane. Yellow crystal. Yield: 0.98 g (81%). m.p. 50 °C. Calculated for C₁₂H₉F₃O₂ (242.20 g·mol⁻¹): C 59.51; H 3.75; F 23.53; O 13.21. Found: C 59.30; H 3.81; F 23.48; O 13.41. ¹H NMR (400 MHz, CDCl₃) δ 15.66 (s, 1H), 7.99 (d, J = 7.8 Hz, 1H), 7.50 (td, J = 7.5, 1.4 Hz, 1H), 7.37 (t, J = 7.4 Hz, 1H), 7.28 – 7.25 (m, 1H), 3.49 (s, 1H), 2.94 – 2.87 (m, 1H), 2.77 (t, J = 6.8 Hz, 1H) (Figure S5). IR (KBr) v_{max}: 2947 cm⁻¹ (s, v_{O-H}), 1600 cm⁻¹ (s, v_{C=O}), 1303 cm⁻¹ (s), 1246 cm⁻¹ (s), 1139 cm⁻¹ (s, v_{C-F}), 753 cm⁻¹ (m, v_{CF₃}) (Figure S6).

3.2. Complex Eu(2-(2,2,2-trifluoroethyl)-1-tetralone)phenanthroline Syntheses

A mixture of 2-(2,2,2-trifluoroethyl)-1-tetralone (0.5 g, 2.06 mmol) and NaOH (0.125 g, 2.06 mmol) in an methanol solvent (15 ml) was stirred for 0.5 h. Another methanol solution (10 ml) of Eu(NO₃)₃·6H₂O (0.31 g, 0.69 mmol) was added dropwise under stirring. To this solution, the 1,10-phenanthroline (0.125 g, 0.69 mmol) was added and allowed to stir for 12 h at room temperature. After removing part of the solvent by reduced pressure distillation, the precipitate formed and filtered off, washed with hexane, and recrystallized with the dichloromethane–hexane.

Single crystals of complex suitable for single-crystal X-ray diffraction study were obtained in about three weeks. Yellow crystal. Yield: 1.73 g (80%). IR (KBr) ν_{max} : 1595 cm^{-1} (s, $\text{v}_{\text{C=O}}$), 1305 cm^{-1} (s), 1233 cm^{-1} (s), 1126 cm^{-1} (s, $\text{v}_{\text{C-F}}$), 755 cm^{-1} (m, v_{CF_3}).

3.3. Complex $\text{Eu}(2\text{-}(2,2,2\text{-trifluoroethyl})\text{-}1\text{-tetralone})_3(\text{Bipyridine})\text{-Hex}$ Syntheses

A methanol solution (10 ml) of $\text{Eu}(\text{NO}_3)_3\text{-}6\text{H}_2\text{O}$ (0.31 g, 0.69 mmol) was added to another mixture methanol solution (15 ml) of 2-(2,2,2-trifluoroethyl)-1-tetralone (0.5 g, 2.06 mmol) and NaOH (0.125 g, 2.06 mmol) under stirring. To this solution, the 2,2'-Bipyridine (0.125 g, 0.69 mmol) was added and allowed to stir for 12 h at room temperature. After removing part of the solvent by reduced pressure distillation, the precipitate formed and filtered off, washed with hexane, and recrystallized with the dichloromethane–hexane. Single crystals of complex suitable for single-crystal X-ray diffraction study were obtained in about three weeks. Yellow crystal. Yield: 0.58 g (75%). IR (KBr) ν_{max} : 1596 cm^{-1} (s, $\text{v}_{\text{C=O}}$), 1307 cm^{-1} (s), 1231 cm^{-1} (s), 1123 cm^{-1} (s, $\text{v}_{\text{C-F}}$), 755 cm^{-1} (m, v_{CF_3}).

3.4. Theoretical Calculations

The DFT-B3LYP method [19] and Time-dependent density functional theory (TDDFT) in the Gaussian 03 software [20] were used to optimize the structure obtained from the X-ray single crystal structure analysis and calculate the absorption properties on the basis of the optimized geometry structures in the excited states. The ECP52MWB basis sets with the effective core potentials (ECPs) [21-22] were used for Eu atoms and 6-31G(d) basis sets for other atoms. No negative frequencies were obtained in frequency calculations of the optimized structures demonstrated that the optimized structures are the energy minimum on the potential energy surfaces.

4. Conclusions

In summary, we reported that two novel eight-coordinated Eu(III) complexes, $\text{Eu}(2\text{-}(2,2,2\text{-trifluoroethyl})\text{-}1\text{-tetralone})_3\text{phenanthroline}$ and $\text{Eu}(2\text{-}(2,2,2\text{-trifluoroethyl})\text{-}1\text{-tetralone})_3(\text{Bipyridine})\text{-Hex}$, which were synthesized by the reaction of 2-(2,2,2-trifluoroethyl)-1-tetralone, containing n-donor ligands (1,10-phenanthroline or 2,2'-Bipyridine) and $\text{Eu}(\text{NO}_3)_3\text{-}6\text{H}_2\text{O}$ in ethanol solution at room temperature. The structure and property of complexes **1-2** were characterized by thermal stability analysis, X-ray single crystal diffraction analysis, IR, UV and fluorescence spectrums study. Structural analysis shows that the tris- β -diketonate Eu³⁺ complexes, each eight-coordinated center Eu³⁺ is chelated with three β -diketonate-type ligands (TFT) and one bidentate containing n-donor ligand (phen or bpy). Luminescence studies revealed that the TFT ligand is an effective sensitizer on luminescence of Eu³⁺ ions due to the ligand transfers the absorbed energy effectively to the emitting level of the center metal ion, and the phen and bpy, acts as a ancillary bidentate nitrogen ligands enhance not only the luminescence property but also thermal stability effectively. The experimental data can be explained with the DFT calculated transitions quite well.

Supplementary Materials: The following are available online at www.mdpi.com/link, Figure S1: Crystal structure of complex **1**, Table S1: Selected bond lengths/ \AA for complex **1**, Table S2: Hydrogen bond lengths/ \AA and bond angles/° for complex **1**, Figure S2: Crystal structure of complex **2**, Table S3: Selected bond lengths/ \AA for complex **2**, Table S4: Hydrogen bond lengths/ \AA and bond angles/° for complex **1**, Figure S3: Schematic energy level diagram for complex **1** (S, excited singlet state; T, excited triplet state), Figure S4: Luminescence

decay profiles for complex **1** (a) and **2** (b) in solid-state were measured at 298K, Figure S5: ^1H NMR analysis of 2-(2,2,2-trifluoroethyl)-1-tetralone, Figure S6: FT-IR spectra of TFT and complexes **1-2**.

Acknowledgments: This project is supported by National Natural Science Foundation of China (No. 50975058), Heilongjiang Province (Nos. B201207 and B201208).

Author Contributions: Yanjun Hou and Haifeng Shao were responsible for conception and design of this study, and Haifeng Shao and Jinyuan Bai synthesized all compounds. Yanjun Hou was responsible for the crystal structure and data analysis, Haijun Niu provided the measurement of fluorescence spectrophotometer, and Haifeng Shao wrote the paper. All authors discuss the manuscript and comment the paper.

Conflicts of Interest: The authors declares no conflicts of interest.

References

1. Carlos, L. D.; Ferreira, R. A.; Bermudez Vde, Z.; Ribeiro, S. J. Lanthanide-containing light-emitting organic-inorganic hybrids: a bet on the future. *Adv Mater* **2009**, *21*, 509-34,
DOI: 10.1002/adma.200801635. Available online: <http://www.ncbi.nlm.nih.gov/pubmed/21161975> (accessed on 2 February 2009).
2. Gangan, T. V. U.; Sreenadh, S.; Reddy, M. L. P. Visible-light excitable highly luminescent molecular plastic materials derived from Eu³⁺-biphenyl based β -diketonate ternary complex and poly(methylmethacrylate). *J Photoch Photobio A* **2016**, *328*, 171-181,
DOI: 10.1016/j.jphotochem.2016.06.005. Available online: <http://dx.doi.org/10.1016/j.jphotochem.2016.06.005> (accessed on 7 June 2016).
3. Congiu, M.; Alamiry, M.; Moudam, O.; Ciorba, S.; Richardson, P. R.; Maron, L.; Jones, A. C.; Richards, B. S.; Robertson, N. Preparation and photophysical studies of [Ln(hfac)₃DPEPO], Ln = Eu, Tb, Yb, Nd, Gd; interpretation of total photoluminescence quantum yields. *Dalton Trans* **2013**, *42*, 13537-45,
DOI: 10.1039/c3dt51380g. Available online: <http://www.ncbi.nlm.nih.gov/pubmed/23900430> (accessed on 7 October 2013).
4. Divya, V.; Sankar, V.; Raghu, K. G.; Reddy, M. L. A mitochondria-specific visible-light sensitized europium beta-diketonate complex with red emission. *Dalton Trans* **2013**, *42*, 12317-23,
DOI: 10.1039/c3dt51117k. Available online: <http://www.ncbi.nlm.nih.gov/pubmed/23852562> (accessed on 5 July 2013).
5. Thibon, A.; Pierre, V. C. Principles of responsive lanthanide-based luminescent probes for cellular imaging. *Anal Bioanal Chem* **2009**, *394*, 107-20,
DOI: 10.1007/s00216-009-2683-2. Available online: <http://www.ncbi.nlm.nih.gov/pubmed/19283368> (accessed on 13 March 2009).
6. Li, D.; Tian, X.; Hu, G.; Zhang, Q.; Wang, P.; Sun, P.; Zhou, H.; Meng, X.; Yang, J.; Wu, J.; Jin, B.; Zhang, S.; Tao, X.; Tian, Y. Synthesis, crystal structures, photophysical properties, and bioimaging of living cells of bis-beta-diketonate phenothiazine ligands and its cyclic dinuclear complexes. *Inorg Chem* **2011**, *50*, 7997-8006,
DOI: 10.1021/ic200150h. Available online: <http://www.ncbi.nlm.nih.gov/pubmed/21827147> (accessed on 9 August 2011).
7. George, T. M.; Sajan, M. J.; Gopakumar, N.; Reddy, M. L. P. Bright red luminescence and triboluminescence from PMMA-doped polymer film materials supported by Eu³⁺-triphenylphosphine based β -diketonate and 4,5-bis(diphenylphosphino)-9,9-dimethylxanthene oxide. *J Photoch Photobio A* **2016**, *317*, 88-99,
DOI: 10.1016/j.jphotochem.2015.11.016. Available online: <http://ir.niist.res.in:8080/jspui/handle/123456789/2388> (accessed on 1 December 2015).
8. Taydakov, I. V.; Akkuzina, A. A.; Avetisov, R. I.; Khomyakov, A. V.; Saifutyarov, R. R.; Avetissov, I. C., Effective electroluminescent materials for OLED applications based on lanthanide 1,3-diketonates bearing pyrazole moiety. *J Lumin* **2016**, *177*, 31-39,
DOI: 10.1016/j.jlumin.2016.04.017. Available online: <http://dx.doi.org/10.1016/j.jlumin.2016.04.017> (accessed on 13 April 2016).

9. Pereira, C. C.; Dias, S.; Coutinho, I.; Leal, J. P.; Branco, L. C.; Laia, C. A. Europium(III) tetrakis(beta-diketonate) complex as an ionic liquid: a calorimetric and spectroscopic study. *Inorg Chem* **2013**, *52*, 3755-64,
DOI: 10.1021/ic3023024. Available online: <http://www.ncbi.nlm.nih.gov/pubmed/23477603>. (accessed on 11 March 2013).

10. Lapaev, D. V.; Nikiforov, V. G.; Safiullin, G. M.; Lobkov, V. S.; Knyazev, A. A.; Krupin, A. S.; Galyametdinov, Y. G. Changes in luminescent properties of vitrified films of terbium(III) β -diketonate complex upon UV laser irradiation. *J Lumin* **2016**, *175*, 106-112,
DOI: 10.1016/j.jlumin.2016.02.006. Available online: <http://dx.doi.org/10.1016/j.jlumin.2016.02.006> (accessed on 15 February 2016).

11. Xie, C.; Wu, L.; Han, J.; Soloshonok, V. A.; Pan, Y. Assembly of Fluorinated Quaternary Stereogenic Centers through Catalytic Enantioselective Detrifluoroacetylation Aldol Reactions. *Angew Chem* **2015**, *54*, 6019-23,
DOI: 10.1002/anie.201500908. Available online: <http://www.ncbi.nlm.nih.gov/pubmed/25808758>. (accessed on 24 March 2015).

12. Joel Bernstein, R. E. D.; Liat Shimon, and Ning-Leh Chang. Patterns in Hydrogen Bonding: Functionality and Graph Set Analysis in Crystals. *Angew. Chem. Int. Ed. Engl* **1995**, *34*, 1555-1573,
DOI: 10.1002/anie.199515551. Available online: <http://onlinelibrary.wiley.com/doi/10.1002/anie.199515551/abstract>. (accessed on 1995 August 8)

13. Xu, H.; Hu, H. C.; Cao, C. S.; Zhao, B., Lanthanide organic framework as a regenerable luminescent probe for Fe(3+). *Inorg Chem* **2015**, *54*, 4585-7,
DOI: 10.1021/acs.inorgchem.5b00113 Available online: <https://www.altmetric.com/details/3976135> (accessed on 247 May 2015).

14. Ahmed, Z.; Iftikhar, K. Solution studies of lanthanide (III) complexes based on 1,1,1,5,5-hexafluoro-2,4-pentanedione and 1,10-phenanthroline Part-I: Synthesis, ^1H NMR, 4f-4f absorption and photoluminescence. *Inorg Chim Acta* **2010**, *363*, 2606-2615,
DOI: 10.1021/jp003937v C. Available online: <http://dx.doi.org/10.1016/j.ica.2010.04.040> (accessed on 10 August 2010).

15. Ma, X.; Li, X.; Cha, Y.-E.; Jin, L.-P. Highly Thermostable One-Dimensional Lanthanide(III) Coordination Polymers Constructed from Benzimidazole-5,6-dicarboxylic Acid and 1,10-Phenanthroline: Synthesis, Structure, and Tunable White-Light Emission. *Cryst Growth Des* **2012**, *12*, 5227-5232.
DOI: 10.1021/cg300932a. Available online: <http://pubs.acs.org/doi/pdfplus/10.1021/cg300932a>. (accessed on 20 September 2012).

16. Ahmed, Z.; Iftikhar, K. Efficient photoluminescent complexes of 400–1800 nm wavelength emitting lanthanides containing organic sensitizers for optoelectronic devices. *RSC Adv.* **2014**, *4*, 63696,
DOI: 10.1039/c4ra11330f. Available online: <http://pubs.rsc.org/en/content/articlehtml/2014/ra/c4ra11330f>. (accessed on 13 November 2014).

17. Armelao, L.; Quici, S.; Barigelli, F.; Accorsi, G.; Bottaro, G.; Cavazzini, M.; Tondello, E. Design of luminescent lanthanide complexes: From molecules to highly efficient photo-emitting materials. *Coordin Chem Rev* **2010**, *254*, 487-505,
DOI: 10.1016/j.ccr.2009.07.025. Available online: <http://www.sciencedirect.com/science/article/pii/S0010854509002069>. (accessed on 7 August 2009).

18. Sheldrick, G.M. *SHELXS-97, Program for the Solution of Crystal Structures*; University of Göttingen: Göttingen, Germany, 1997,

19. Matsuzawa N. N.; Ishitani. Time-Dependent Density Functional Theory Calculations of Photoabsorption Spectra in the Vacuum Ultraviolet Region. *J. Phys. Chem. A* **2001**, *226*, 4953,
DOI: 10.1002/1521-3951(200107)226:1<69::AID-PSSB69>3.0.CO;2-7. Available online: <http://www.osti.gov/scitech/biblio/15005499>. (accessed on 30 May 2001).

20. Frisch, M.-J.; Trucks, G.-W.; Schlegel, H.-B.; Scuseria, G.-E.; Robb, M.-A.; Cheeseman, J.-R.; Montgomery, J.-A., Jr.; Vreven, T.; Kudin, K.-N.; Burant, J.-C.; et al. Gaussian 03Revision C.01; Gaussian Inc.: Wallingford, CT, USA, 2004.

21. Dolg, M.; Stoll, H.; Savin, A.; Preuss, H. Pseudopotential study of the rare earth monohydrides, monoxides and monofluorides. *Theor Chim Acta* **1989**, *75*, 369-387,

DOI: 10.1007/BF00526695. Available online: <http://link.springer.com/article/10.1007%2FBF00526695>. (accessed on 3 October 1988).

22. Dolg, M.; Stoll, H.; Preuss, H. A combination of quasirelativistic pseudopotential and ligand field calculations for lanthanoid compounds. *Theor Chim Acta* **1993**, *85*, 441-450,
DOI: 10.1007/BF01112983. Available online: <http://link.springer.com/article/10.1007%2FBF01112983> (accessed on 12 October 1992).



© 2017 by the authors; licensee *Preprints*, Basel, Switzerland. This article is an open access article distributed under the terms and conditions of the Creative Commons by Attribution (CC-BY) license (<http://creativecommons.org/licenses/by/4.0/>).